

Published in final edited form as:

*Cell Rep.* 2012 February 23; 1(2): 83–90. doi:10.1016/j.celrep.2011.12.008.

## Histone H3R2 symmetric dimethylation and histone H3K4 trimethylation are tightly correlated in eukaryotic genomes

Chih-Chi Yuan<sup>1,\*</sup>, Adam G.W. Matthews<sup>1,4,\*</sup>, Yi Jin<sup>2,\*</sup>, Chang Feng Chen<sup>1</sup>, Brad A. Chapman<sup>1,5</sup>, Toshiro K. Ohsumi<sup>1</sup>, Karen C. Glass<sup>3,6</sup>, Tatiana G. Kutateladze<sup>3</sup>, Mark L. Borowsky<sup>1</sup>, Kevin Struhl<sup>2</sup>, and Marjorie A. Oettinger<sup>1,+</sup>

<sup>1</sup>Department of Molecular Biology, Massachusetts General Hospital and Department of Genetics, Harvard Medical School, Boston, MA 02114 USA

<sup>2</sup>Department of Biological Chemistry and Molecular Pharmacology, Harvard Medical School, Boston, MA 02115 USA

<sup>3</sup>Department of Pharmacology, University of Colorado Denver, Aurora, CO 80045 USA

### Summary

The preferential *in vitro* interaction of the PHD finger of RAG2, a subunit of the V(D)J recombinase, with histone H3 tails simultaneously trimethylated at lysine 4 and symmetrically dimethylated at arginine 2 (H3R2me2sK4me3) predicted the existence of the previously unknown histone modification, H3R2me2s. Here, we report the *in vivo* identification of H3R2me2s. Consistent with the binding specificity of the RAG2 PHD finger, high levels of H3R2me2sK4me3 are found at antigen receptor gene segments ready for rearrangement. However, this double modification is much more general; it is conserved throughout eukaryotic evolution. In mouse, H3R2me2s is tightly correlated with H3K4me3 at active promoters throughout the genome. Mutational analysis in *S. cerevisiae* reveals that deposition of H3R2me2s requires the same Set1 complex that deposits H3K4me3. Our work suggests that H3R2me2sK4me3, not simply H3K4me3 alone, is the mark of active promoters, and that factors that recognize H3K4me3 will have their binding modulated by their preference for H3R2me2s.

### Introduction

Multiple mechanisms ensure that the V(D)J recombination events required to assemble antigen receptor genes occur in a lineage-, stage-, and allele-specific manner, with DNA double-strand breaks targeted only to the appropriate antigen receptor loci, and not elsewhere in the genome. Multiple histone tail modifications are associated with antigen

Crown Copyright © 2011 Published by Elsevier Inc. All rights reserved.

\*Contact: oettinger@frodo.mgh.harvard.edu; 617-726-5967 (p); 617-726-5949 (f).

<sup>4</sup>Present address: Howard Hughes Medical Institute, Department of Biology, Massachusetts Institute of Technology, Cambridge, MA 02139 USA

<sup>5</sup>Present address: Center for Health Bioinformatics, Harvard School of Public Health, Boston, MA 02115 USA

<sup>6</sup>Present address: Department of Pharmaceutical Sciences, Albany College of Pharmacy and Health Sciences, Colchester, VT 05446 USA

\*These authors contributed equally to the work.

**Publisher's Disclaimer:** This is a PDF file of an unedited manuscript that has been accepted for publication. As a service to our customers we are providing this early version of the manuscript. The manuscript will undergo copyediting, typesetting, and review of the resulting proof before it is published in its final citable form. Please note that during the production process errors may be discovered which could affect the content, and all legal disclaimers that apply to the journal pertain.

### Accession Numbers

The GEO accession number for the ChIP-seq data reported in this paper is GSE35316.

receptor loci, with activating modifications being found at loci poised to rearrange, and modifications characteristic of heterochromatin found at inactive loci (Gellert, 2002; Hesslein and Schatz, 2001; Jung et al., 2006; Matthews and Oettinger, 2009).

Although the specific function of most of these histone tail modifications remains to be determined, recent work has shed light on the role of H3K4me3 in V(D)J recombination. H3K4me3 is enriched at antigen receptor loci that are poised to carry out recombination (Ji et al., 2010; Matthews et al., 2007; Perkins et al., 2004; Xu and Feeney, 2009). Our structural analysis showed that the PHD finger of RAG2 specifically binds H3K4me3. Introducing point mutations in any of three crucial amino acids in the PHD finger or globally reducing H3K4me3 levels dramatically decreases recombination at the IgH locus in pro-B cell lines (Matthews et al., 2007).

The role of H3K4me3 in V(D)J recombination is not simply to tether RAG2 to its target sites. In the absence of H3K4me3-binding, the C-terminal regulatory domains of RAG1 and RAG2 interact to inhibit V(D)J cleavage. Binding of H3K4me3 to the RAG2 PHD finger alleviates this inhibition (Grundy et al., 2010). Thus, the interaction of RAG2 with an epigenetic modification alters the catalytic properties of the RAG complex to regulate its activity.

The crystal structure of the RAG2 PHD finger complexed with H3K4me3 peptide revealed an additional binding pocket that could accommodate methylated H3R2. Arginine residues can be either monomethylated, symmetrically dimethylated, or asymmetrically dimethylated. We found that the RAG2-PHD domain preferentially binds the H3 tail when it is symmetrically dimethylated on R2 and trimethylated on K4. Indeed, a 20-fold increase in binding affinity, as measured by fluorescence anisotropy, is observed when the dual modification (H3R2me2sK4me3) is present as compared to H3K4me3 alone (Table S1).

The symmetrical dimethylation of Arg2 of histone H3 has not previously been described. The preference of RAG2 for H3R2me2sK4me3 suggested that H3R2me2s might exist in vivo and that it might colocalize with H3K4me3 at antigen receptor loci poised to undergo V(D)J recombination. By contrast, asymmetrically dimethylated arginine 2 (H3R2me2a) and H3K4me3 are mutually exclusive modifications. Here we show that the novel histone modification, H3R2me2s, is tightly correlated with H3K4me3 not only at IgH, but throughout the mouse genome. Genetic experiments in *S. cerevisiae* demonstrate an intimate relationship between H3R2me2s and H3K4me3, with the deposition of H3R2me2s dependent on the COMPASS complex that carries out H3K4 methylation. These findings expand the role of H3R2 in the metabolism of H3K4 and define H3R2me2sK4me3 as a mark of active promoters.

## Results and Discussion

### H3R2me2s is present at recombinationally active antigen receptor loci

To determine whether H3R2 is symmetrically dimethylated in mammalian cells and to explore the relationship between H3K4me3 and H3R2me2s, we generated two affinity-purified antibodies. The specificity of each affinity-purified antiserum was validated by peptide dot blot analysis (Figure S1A). The first antibody,  $\alpha$ -pan-H3R2me2s, showed >25 fold preference toward H3R2me2s over H3R2me2a and ~5 fold preference for H3R2me2s over H3R2me2sK4me3 (Figure S1A, top left panel). The second antibody,  $\alpha$ -H3R2me2sK4me3, recognized only the H3R2me2sK4me3 peptide and not either modification alone (Figure S1A, bottom left panel).

Both antibodies robustly recognized histone H3 in Western blot analysis of nuclear extracts derived from a lymphoid cell line poised to carry out V(D)J recombination between the IgH D and J segments (Figure S1B). Peptide competition Western blots of the pro-B cell nuclear extracts confirmed that the histone H3 signal was due to bona fide recognition of H3R2me2s and/or H3R2me2sK4me3 (Figure S1C). Chromatin immunoprecipitation followed by qPCR (ChIP-qPCR) revealed that H3R2me2s, H3K4me3, and H3R2me2sK4me3 are all enriched at actively rearranging gene segments in developing lymphoid cells (Figure 1). Thus, H3R2me2s is a novel histone modification present in developing lymphoid cells. Moreover, because the H3R2me2sK4me3 antibody has the unusual property of requiring the simultaneous recognition of two histone modifications, H3R2me2s and H3K4me3 must reside on the same histone tail, at least on some histones, providing an opportunity for RAG2 to simultaneously bind to both methylated residues.

### H3R2me2s colocalizes with H3K4me3 throughout the mouse genome

The striking similarity between the patterns of enrichment observed for the pan-H3R2me2s, H3K4me3, and H3R2me2sK4me3 antibodies (Figure 1 and (Matthews et al., 2007)) suggested that H3R2me2s may be associated with H3K4me3. Indeed, this turns out to be true. We used antibodies to H3K4me3, pan-H3R2me2s, and H3R2me2sK4me3 to perform genome-wide localization analysis (ChIP-seq) in RAG2<sup>-/-</sup> Abelson-transformed pro-B cells. In fact, H3R2me2s and H3R2me2sK4me3 both showed a remarkable genome-wide colocalization with H3K4me3. An example is shown for a gene-rich 350 kb region of murine chromosome 19, where these modifications showed very similar patterns of enrichment, generally localizing to the 5' end of genes (Figure 2A). A closer look at the transcriptional start site (TSS) of a representative gene in this region (Dpf2) revealed that H3R2me2s and H3R2me2sK4me3 are both enriched just upstream and just downstream of the TSS, in a pattern that is nearly identical to the enrichment pattern of H3K4me3 (Figure 2B).

The enrichment of H3R2me2s and H3R2me2sK4me3 flanking genic transcriptional start sites and the correlation of enrichment with gene expression appears to be general. We stratified all annotated mouse genes into four quartiles according to their expression levels in pro-B cells (Gene Expression Omnibus: GSE15330) (Ng et al., 2009) and analyzed the signal intensity for pan-H3R2me2s, H3R2me2sK4me3, and H3K4me3 over a 4 kb window centered on the TSS of these genes. Consistent with previous findings (Barski et al., 2007; Pan et al., 2007), H3K4me3 is found in two peaks flanking the TSS and its enrichment is positively correlated with gene expression (Figure 2C, left panel). Nearly identical patterns were observed for H3R2me2s (Figure 2C, right panel) and H3R2me2sK4me3 (Figure 2C, center panel).

Consistent with the ChIP-qPCR results (Figure 1), H3K4me3, H3R2me2s, and H3R2me2sK4me3 are tightly correlated at the IgH locus (Figure 2D), showing broad enrichment covering the region from DQ52 through the JH cluster, with very few sites of enrichment in the VH domain (Figure S2).

The ChIP-seq results were further validated by qPCR of 60 randomly selected promoters (Table S2) after immunoprecipitation of chromatin from the same RAG2<sup>-/-</sup> Abelson-transformed pro-B cells with the pan-H3R2me2s, H3R2me2sK4me3, or H3K4me3 antibodies. The pair-wise combination shown in Figure 2E displays a strong positive correlation for all sites. Thus, H3R2me2s and H3K4me3 are tightly colocalized throughout the mouse genome.

### H3R2me2s is conserved throughout evolution

To assess the evolutionary conservation of this modification, nuclear extracts from human (*Homo sapiens* - Hs), mouse (*Mus musculus* - Mm), frog (*Xenopus laevis* - Xl), fruit fly (*Drosophila melanogaster* - Dm), and budding yeast (*Saccharomyces cerevisiae* - Sc) cells were tested by Western blot analysis. A strong signal was observed for all of these organisms with both the pan-H3R2me2s and the H3R2me2sK4me3 antibodies (Figure 3A). Thus, H3R2me2s is conserved throughout evolution, as far back as budding yeast. Moreover, the strong signal observed with the H3R2me2sK4me3 antibody, which requires the presence of both modifications on the same histone tail, indicates that colocalization of H3R2me2s and H3K4me3 is conserved to some extent throughout evolution.

### H3R2me2s colocalizes with H3K4me3 in *S. cerevisiae*

We used previously published primer sets to interrogate the distribution pattern of these three modifications at the 5' and 3' ends of representative genes in *S. cerevisiae*: highly transcribed (YLR340W), moderately transcribed (YPR112C and YLR342W), and inactive genes (YPL017C). We observed a striking correlation between the distribution patterns of H3R2me2s, H3K4me3, and H3R2me2sK4me3 (Figure 3B). All three modifications were present at both the 5' and 3' ends of the highly transcribed gene (left panel), enriched at the 5' end of moderately transcribed genes (middle 2 panels), and poorly enriched at an inactive gene (right panel). The primer sets and genes chosen for this analysis are the same that were previously analyzed by ChIP-qPCR for H3R2me2a (Kirmizis et al., 2007). Therefore, in *S. cerevisiae*, H3R2me2s is colocalized with H3K4me3 and anti-correlated with H3R2me2a.

### H3K4 is required for H3R2me2s deposition

Mutating arginine-2 of histone H3 to alanine (H3R2A) has been shown to completely abolish trimethylation of H3K4 (Kirmizis et al., 2007). Given the tight correlation between H3R2me2s and H3K4me3, we asked whether the converse would be true. As shown in Figure 3C, lane 19 we found that no H3R2me2s was detected by Western blot when H3K4 was mutated to alanine (Figure 3C, lane 19). This was not simply due to an inability of the pan-H3R2me2s antibody to recognize its epitope when lysine 4 is mutated to alanine (Figure 3D). Thus H3K4, either unmethylated or in one of its methylated states, is required for H3R2me2s deposition.

### Set1 is required for H3R2me2s deposition

In order to identify the methyltransferase responsible for depositing H3R2me2s, we first used a candidate gene approach, expressing shRNA to all known type II arginine methyltransferases in murine cells. Although levels of the methyltransferases were reduced, a reproducible loss of H3R2me2s modification was not obtained (Figure S3). We then turned to *S. cerevisiae* using Western blot analysis with the pan-H3R2me2s antibody to screen six yeast proteins that have a SET domain and nine proteins that contain putative SAM-binding domains (Figure 3C). Surprisingly, the set1 $\Delta$  strain showed a complete loss of H3R2me2s signal (Figure 3C, lane 2). Since Set1 is the catalytic subunit of COMPASS, the yeast H3K4 methyltransferase, these results suggest two possibilities that are not mutually exclusive: either Set1 is also the catalytic subunit of the H3R2 symmetric dimethyltransferase, or H3K4 methylation is required for H3R2 symmetric dimethylation. The requirement of H3K4 for H3R2me2s deposition is consistent with either interpretation, as H3K4 is required for Set1 binding.

### H3R2me2s deposition is greatly reduced in the absence of H3K4me3

Since Set1 is required for mono-, di-, and tri-methylation of H3K4, we analyzed two additional COMPASS mutants, first to confirm that COMPASS is required for H3R2me2s

deposition, and second to determine whether a particular K4 methylation state is required. Loss of SWD3 (CPS30) – which destabilizes the COMPASS complex and causes the loss of all H3K4 methylation states – caused a complete loss of H3R2me2s (Figure 3E, lane 4). Since the *swd3* strain (Figure 3E, lane 4) exhibits the same phenotype as the *set1Δ* strain (Figure 3E, lane 2), we conclude that the loss of H3R2me2s in the *set1Δ* strain is likely due to loss of COMPASS activity. We then asked if the loss of SPP1 (CPS40), a COMPASS subunit required for the transition from H3K4me2 to H3K4me3, affected H3R2me2s levels. Loss of SPP1 caused a dramatic reduction in the levels of H3R2me2s (Figure 3E, lane 3). Therefore, either H3K4me3 is required for an H3R2 symmetric dimethyltransferase (distinct from COMPASS) to deposit H3R2me2s, or COMPASS is the H3R2 symmetric dimethyltransferase.

### What are the functional roles of H3R2me2s?

The conservation of H3R2me2s and its colocalization with H3K4me3 raises a number of issues. Why are active promoters marked simultaneously by both H3R2me2s and H3K4me3, and what is the function of H3R2me2s? Perhaps H3R2me2s modifies specificities among the multiple H3K4me3-binding proteins. It has remained a puzzle how specificity is achieved when many different proteins recognize H3K4me3. Their ability to bind H3R2me2sK4me3 may be more variable, with the binding of some factors enhanced by the H3R2me2s modification (as with RAG2) while others merely tolerate its presence, and still others may be inhibited (Ramon-Maiques et al., 2007). In this way, fine-tuning of target site recognition could be achieved, with the contribution of multiple interactions required to achieve the ultimate target site specificity. While RAG2 is the only protein currently known to preferentially bind H3R2me2sK4me3, this may simply reflect the novelty of this modification.

Of note, while we have shown that H3R2me2s and H3K4me3 coexist on individual histone tails at promoters, we cannot rule out the possibility that some nucleosomes contain only one or the other modification (perhaps having had one of the two modifications removed), and these nucleosomes could be recognized by different factors. However, the tight genome-wide correlation between H3R2me2s, H3K4me3, and H3R2me2sK4me3 enrichment levels argues that these two modifications are generally found together on the same histone tail.

An additional possible role for H3R2me2s is in the metabolism of H3K4me3. Previous work in yeast and humans has shown that H3K4me3 and H3R2me2a are mutually exclusive histone modifications (Guccione et al., 2007; Hyllus et al., 2007; Kirmizis et al., 2007). Since symmetric dimethylation of H3R2 would preclude asymmetric dimethylation of this residue, H3R2me2s could facilitate or stabilize the trimethylation of H3K4 by protecting the H3K4me3 methyltransferase binding site from being occluded via asymmetric dimethylation of H3R2. H3R2me2s could also serve to maintain H3K4me3 by preventing demethylases from acting at H3K4. In any event, it is clear from their localization patterns that symmetric and asymmetric methylation of H3R2 serve distinct functions in the cell.

### Histone cross-talk

It is increasingly clear that there is a complex interplay between histone modifications. In some cases, one histone modification affects the ability to modify another residue on the same histone (Cheung et al., 2000; Daujat et al., 2002; Guccione et al., 2007; Hyllus et al., 2007; Kirmizis et al., 2007; Lo et al., 2000). In other cases, the modification of one histone affects the modification of another histone in the same nucleosome (Carrozza et al., 2005; Dover et al., 2002; Kim et al., 2009; Ng et al., 2002; Sun and Allis, 2002). Histone modifications can also function to combinatorially regulate the binding of chromatin-associated proteins. For example, HP1 binds H3K9me3 only in the absence of H3S10p

(Fischle et al., 2005)). Modifications on different histone tails within the same mononucleosome can also regulate factor binding in cases where a single chromatin binding protein contains multiple histone recognition domains (e.g. BPTF (Ruthenburg et al., 2011)).

H3R2me2sK4me3 appears to provide another distinct example of histone crosstalk in which the two modifications influence each other's deposition as well as subsequent factor binding. Here H3R2me2s and H3K4me3 are two nearby residues on the same histone tail that appear to always co-exist (though we cannot rule out the possibility that there are developmental or regulated states where they are separate). Thus, rather than affecting binding of a factor in a binary way (as with HP1 binding H3K9me3 but not H3K9me3S10p (Fischle et al., 2005)), it appears that all H3K4me3 binders whose binding domains encompass H3R2 will be influenced by the modification state of H3R2. Moreover, either H3R2me2s and H3K4me3 are dependent on the same histone methyltransferase complex (see below) and/or the deposition of H3R2me2s is dependent on the prior deposition of H3K4me3. Thus, we have uncovered a striking new example of the complexity of histone crosstalk.

### Interplay between H3K4 and H3R2 methylation

The tight correlation of H3R2me2s and H3K4me3 leads to the obvious questions: what role does H3R2 play in H3K4 trimethylation and what role does H3K4 trimethylation play in H3R2 symmetric dimethylation, what enzymatic machinery is responsible for depositing H3R2me2s, and how are the two events linked? As mentioned above, it is known that the presence of H3R2 is itself required for H3K4 trimethylation (Kirmizis et al., 2007), an observation which we have independently confirmed. One simple model is that either H3R2me0 or H3R2me1 is required for SPP1 binding, which in turn is required for H3K4 trimethylation, followed by methylation of H3R2 on the same histone tail, either by COMPASS or by a distinct H3K4me3-dependent H3R2 methyltransferase. Alternatively, COMPASS could bind to H3R2, either in its unmodified or its mono-methylated form, and first catalyze the symmetric dimethylation of H3R2 and then the trimethylation of H3K4. Both of these models are consistent with our findings that Set1 and Spp1 are required for the generation of H3R2me2s, and the previous observations that H3K4me3 is lost in an H3R2A mutant yeast strains and that Spp1 is highly enriched at sites of H3K4me3 (and therefore, also H3R2me2s and H3R2me2sK4me3) and absent from regions enriched for H3R2me2a (Kirmizis et al., 2007). These findings also underscore the yin-yang relationship between H3R2me2a and H3R2me2s.

It is worth noting that a number of yeast phenotypes associated with the mutation of H3R2 to alanine have been described. At present, it is impossible to determine whether these phenotypes, including the delayed activation of GAL genes and the loss of silencing in the *HMR*, *HML*, telomere and *rDNA* loci, reflect the loss of H3R2me2s, H3R2me2a, or H3K4me3, or simply the loss of arginine.

In summary, the tight coupling of H3R2me2s and H3K4me3 is yet another example of the intricate interactions between histone modifications. The impetus for actively seeking evidence that H3R2me2s exists came from predictions based on our prior biochemical studies of the RAG2 PHD finger. We believe this is the first example of a histone modification being sought and identified based on structural and biochemical analyses of a histone recognition domain. The finding that active promoters are marked by H3R2me2sK4me3 will now lead to a rethinking of how the H3R2me2s modification impacts the various H3K4me3 binding proteins, and the importance of proteins like UHRF that solely recognize H3R2 uninfluenced by the H3K4 methylation status.

## Experimental Procedures

### Antibody generation

To generate an  $\alpha$ -pan-H3R2me2s antibody, rabbits were immunized with H3R2me2s(1–10) conjugated to KLH. Antiserum from each rabbit was immunodepleted with H3(1–10) and H3R2me2a(1–10), then affinity-purified with H3R2me2s(1–10). All four antisera were characterized separately.

To generate an  $\alpha$ -H3R2me2sK4me3 antibody, rabbits were immunized with H3R2me2sK4me3(1–10) conjugated to KLH. Antiserum from each rabbit was immunodepleted with H3R2me2a(1–10) and H3K4me3(1–10), then affinity-purified with H3R2me2sK4me3(1–10). All four antisera were characterized separately.

### Antibody characterization

Peptide dot-blotting was performed essentially as described previously (Perez-Burgos et al., 2004).

Western blots were performed according to standard procedures. See Supplementary Experimental Methods for details.

### Antibodies

Commercial antibodies used in this study include  $\alpha$ -H3 (Abcam ab1791),  $\alpha$ -H4 (Abcam ab31827),  $\alpha$ -H3K4me3 (Abcam ab8580), and  $\alpha$ -Pol II (Covance 8WG16).

### Chromatin immunoprecipitation

Chromatin immunoprecipitation (ChIP) was carried out essentially as described previously (Ciccone et al., 2004; Fan et al., 2008; Fan et al., 2010). qPCR was performed using the primers listed in Table S2. Deep sequencing was performed on an Illumina Genome Analyzer. Library generation was performed according to manufacturer's recommendations. See Supplementary Experimental Methods for details.

### Bioinformatics analysis

Sequence processing and transcriptional start site analysis were performed according to standard procedures. See Supplementary Experimental Methods for details.

### PRMT screening

Lentiviruses carrying shRNA toward PRMT5, 7, and 10 were generated as described previously (Moffat et al., 2006). Transduction, selection, RT-qPCR, and Western blotting were performed according to standard procedures. See Supplementary Experimental Methods for details.

## Supplementary Material

Refer to Web version on PubMed Central for supplementary material.

## Acknowledgments

We would like to thank Yu-Hui Chen for assistance with statistical analysis, Sandhya Pulivarthy for assistance with shRNA experiments, Mark Parthun and Fred Winston for mutant yeast strains, Zarnik Moqtaderi for assisting in the generation of yeast nuclear extracts, Jose Antao for *Drosophila* S2 cells, and Mike Blower for *Xenopus* heart tissue. This work was supported by National Institutes of Health grants GM048026 (MAO), DK082711 (MAO), AI083510 (MAO), CA113472 (TGK), and GM30186 (KS). A.G.W.M. was a Damon Runyon Fellow supported by

the Damon Runyon Cancer Research Foundation (DRG-1994-08). KCG was supported by an NIH NRSA Postdoctoral Fellowship (KCG).

## References

- Barski A, Cuddapah S, Cui K, Roh TY, Schones DE, Wang Z, Wei G, Chepelev I, Zhao K. High-resolution profiling of histone methylations in the human genome. *Cell*. 2007; 129:823–837. [PubMed: 17512414]
- Carrozza MJ, Li B, Florens L, Suganuma T, Swanson SK, Lee KK, Shia WJ, Anderson S, Yates J, Washburn MP, et al. Histone H3 methylation by Set2 directs deacetylation of coding regions by Rpd3S to suppress spurious intragenic transcription. *Cell*. 2005; 123:581–592. [PubMed: 16286007]
- Cheung P, Tanner KG, Cheung WL, Sassone-Corsi P, Denu JM, Allis CD. Synergistic coupling of histone H3 phosphorylation and acetylation in response to epidermal growth factor stimulation. *Mol Cell*. 2000; 5:905–915. [PubMed: 10911985]
- Ciccone DN, Morshead KB, Oettinger MA. Chromatin immunoprecipitation in the analysis of large chromatin domains across murine antigen receptor loci. *Methods Enzymol*. 2004; 376:334–348. [PubMed: 14975316]
- Daujat S, Bauer UM, Shah V, Turner B, Berger S, Kouzarides T. Crosstalk between CARM1 methylation and CBP acetylation on histone H3. *Curr Biol*. 2002; 12:2090–2097. [PubMed: 12498683]
- Dover J, Schneider J, Tawiah-Boateng MA, Wood A, Dean K, Johnston M, Shilatifard A. Methylation of histone H3 by COMPASS requires ubiquitination of histone H2B by Rad6. *J Biol Chem*. 2002; 277:28368–28371. [PubMed: 12070136]
- Fan X, Lamarre-Vincent N, Wang Q, Struhl K. Extensive chromatin fragmentation improves enrichment of protein binding sites in chromatin immunoprecipitation experiments. *Nucleic acids research*. 2008; 36:e125. [PubMed: 18765474]
- Fan X, Moqtaderi Z, Jin Y, Zhang Y, Liu XS, Struhl K. Nucleosome depletion at yeast terminators is not intrinsic and can occur by a transcriptional mechanism linked to 3'-end formation. *Proceedings of the National Academy of Sciences of the United States of America*. 2010; 107:17945–17950. [PubMed: 20921369]
- Fischle W, Tseng BS, Dormann HL, Ueberheide BM, Garcia BA, Shabanowitz J, Hunt DF, Funabiki H, Allis CD. Regulation of HP1-chromatin binding by histone H3 methylation and phosphorylation. *Nature*. 2005; 438:1116–1122. [PubMed: 16222246]
- Gellert M. V(D)J recombination: RAG proteins, repair factors, and regulation. *Annu Rev Biochem*. 2002; 71:101–132. [PubMed: 12045092]
- Grundy GJ, Yang W, Gellert M. Autoinhibition of DNA cleavage mediated by RAG1 and RAG2 is overcome by an epigenetic signal in V(D)J recombination. *Proc Natl Acad Sci U S A*. 2010; 107:22487–22492. [PubMed: 21149691]
- Guccione E, Bassi C, Casadio F, Martinato F, Cesaroni M, Schuchlantz H, Luscher B, Amati B. Methylation of histone H3R2 by PRMT6 and H3K4 by an MLL complex are mutually exclusive. *Nature*. 2007; 449:933–937. [PubMed: 17898714]
- Hesslein DG, Schatz DG. Factors and forces controlling V(D)J recombination. *Adv Immunol*. 2001; 78:169–232. [PubMed: 11432204]
- Hyllus D, Stein C, Schnabel K, Schiltz E, Imhof A, Dou Y, Hsieh J, Bauer UM. PRMT6-mediated methylation of R2 in histone H3 antagonizes H3 K4 trimethylation. *Genes Dev*. 2007; 21:3369–3380. [PubMed: 18079182]
- Ji Y, Resch W, Corbett E, Yamane A, Casellas R, Schatz DG. The in vivo pattern of binding of RAG1 and RAG2 to antigen receptor loci. *Cell*. 2010; 141:419–431. [PubMed: 20398922]
- Jung D, Giallourakis C, Mostoslavsky R, Alt FW. Mechanism and control of V(D)J recombination at the immunoglobulin heavy chain locus. *Annu Rev Immunol*. 2006; 24:541–570. [PubMed: 16551259]
- Kim J, Guermah M, McGinty RK, Lee JS, Tang Z, Milne TA, Shilatifard A, Muir TW, Roeder RG. RAD6-Mediated transcription-coupled H2B ubiquitylation directly stimulates H3K4 methylation in human cells. *Cell*. 2009; 137:459–471. [PubMed: 19410543]



- Kirmizis A, Santos-Rosa H, Penkett CJ, Singer MA, Vermeulen M, Mann M, Bahler J, Green RD, Kouzarides T. Arginine methylation at histone H3R2 controls deposition of H3K4 trimethylation. *Nature*. 2007; 449:928–932. [PubMed: 17898715]
- Lo WS, Trievel RC, Rojas JR, Duggan L, Hsu JY, Allis CD, Marmorstein R, Berger SL. Phosphorylation of serine 10 in histone H3 is functionally linked in vitro and in vivo to Gcn5-mediated acetylation at lysine 14. *Mol Cell*. 2000; 5:917–926. [PubMed: 10911986]
- Matthews AG, Kuo AJ, Ramon-Maiques S, Han S, Champagne KS, Ivanov D, Gallardo M, Carney D, Cheung P, Ciccone DN, et al. RAG2 PHD finger couples histone H3 lysine 4 trimethylation with V(D)J recombination. *Nature*. 2007; 450:1106–1110. [PubMed: 18033247]
- Matthews AG, Oettinger MA. RAG: a recombinase diversified. *Nat Immunol*. 2009; 10:817–821. [PubMed: 19621044]
- Moffat J, Grueneberg DA, Yang X, Kim SY, Kloepfer AM, Hinkle G, Piqani B, Eisenhaure TM, Luo B, Grenier JK, et al. A lentiviral RNAi library for human and mouse genes applied to an arrayed viral high-content screen. *Cell*. 2006; 124:1283–1298. [PubMed: 16564017]
- Ng HH, Xu RM, Zhang Y, Struhl K. Ubiquitination of histone H2B by Rad6 is required for efficient Dot1-mediated methylation of histone H3 lysine 79. *J Biol Chem*. 2002; 277:34655–34657. [PubMed: 12167634]
- Ng SY, Yoshida T, Zhang J, Georgopoulos K. Genome-wide lineage-specific transcriptional networks underscore Ikaros-dependent lymphoid priming in hematopoietic stem cells. *Immunity*. 2009; 30:493–507. [PubMed: 19345118]
- Pan G, Tian S, Nie J, Yang C, Ruotti V, Wei H, Jonsdottir GA, Stewart R, Thomson JA. Whole-genome analysis of histone H3 lysine 4 and lysine 27 methylation in human embryonic stem cells. *Cell Stem Cell*. 2007; 1:299–312. [PubMed: 18371364]
- Perez-Burgos L, Peters AH, Opravil S, Kauer M, Mechtler K, Jenuwein T. Generation and characterization of methyl-lysine histone antibodies. *Methods in enzymology*. 2004; 376:234–254. [PubMed: 14975310]
- Perkins EJ, Kee BL, Ramsden DA. Histone 3 lysine 4 methylation during the pre-B to immature B-cell transition. *Nucleic Acids Res*. 2004; 32:1942–1947. [PubMed: 15051812]
- Ramon-Maiques S, Kuo AJ, Carney D, Matthews AG, Oettinger MA, Gozani O, Yang W. The plant homeodomain finger of RAG2 recognizes histone H3 methylated at both lysine-4 and arginine-2. *Proc Natl Acad Sci U S A*. 2007; 104:18993–18998. [PubMed: 18025461]
- Ruthenburg AJ, Li H, Milne TA, Dewell S, McGinty RK, Yuen M, Ueberheide B, Dou Y, Muir TW, Patel DJ, et al. Recognition of a mononucleosomal histone modification pattern by BPTF via multivalent interactions. *Cell*. 2011; 145:692–706. [PubMed: 21596426]
- Sun ZW, Allis CD. Ubiquitination of histone H2B regulates H3 methylation and gene silencing in yeast. *Nature*. 2002; 418:104–108. [PubMed: 12077605]
- Xu CR, Feeney AJ. The epigenetic profile of Ig genes is dynamically regulated during B cell differentiation and is modulated by pre-B cell receptor signaling. *J Immunol*. 2009; 182:1362–1369. [PubMed: 19155482]

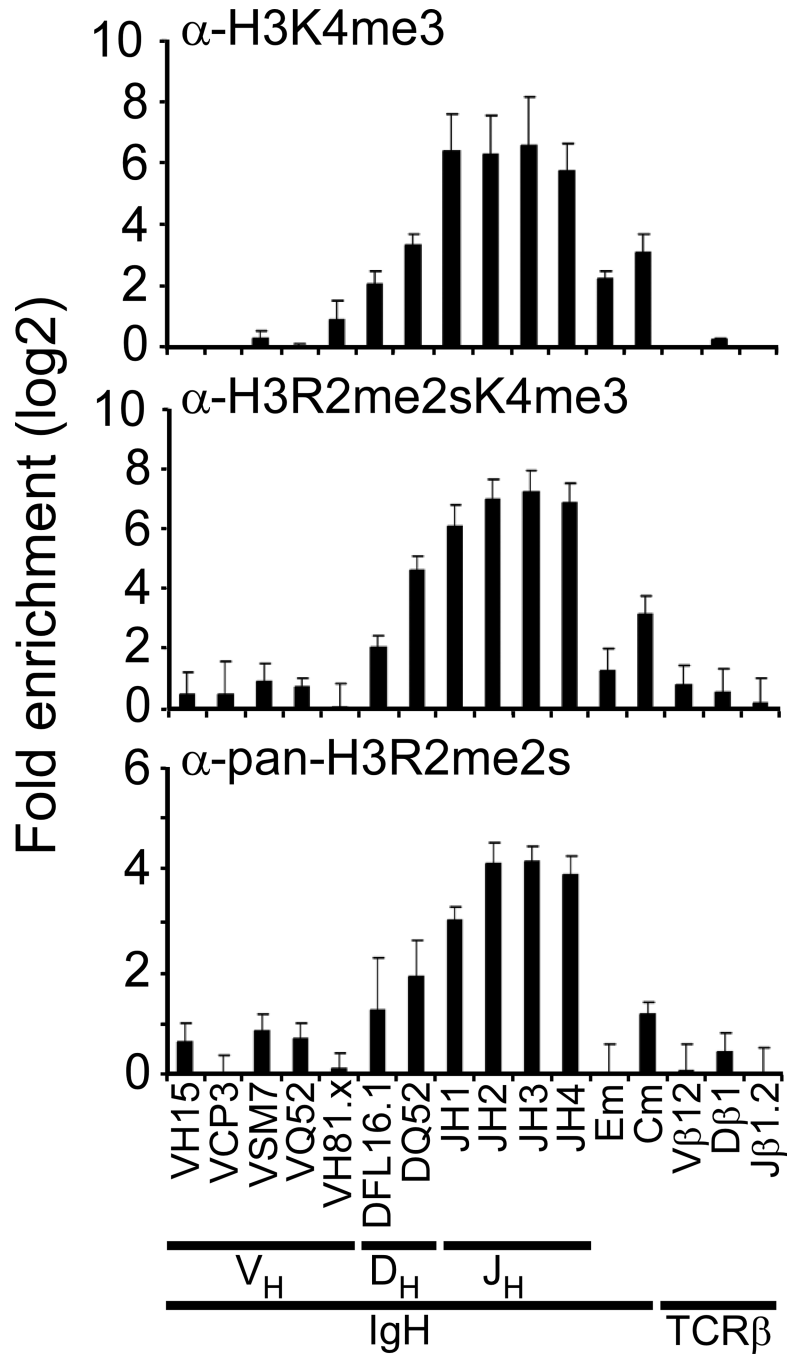


**Figure 1.** H3R2me2s colocalizes with H3K4me3 at the IgH locus in Rag2<sup>-/-</sup> pro-B cells. Chromatin from Rag2<sup>-/-</sup> Abelson-transformed pro-B cells was immunoprecipitated with the  $\alpha$ -H3K4me3 (upper panel),  $\alpha$ -H3R2me2sK4me3 (middle panel), or  $\alpha$ -pan-H3R2me2s (lower panel) antibodies. The enrichment of each modification relative to histone H3 was examined by qPCR using primers that span the IgH and TCR $\beta$  loci. Results represent the mean  $\pm$  S.D. of at least two independent experiments.

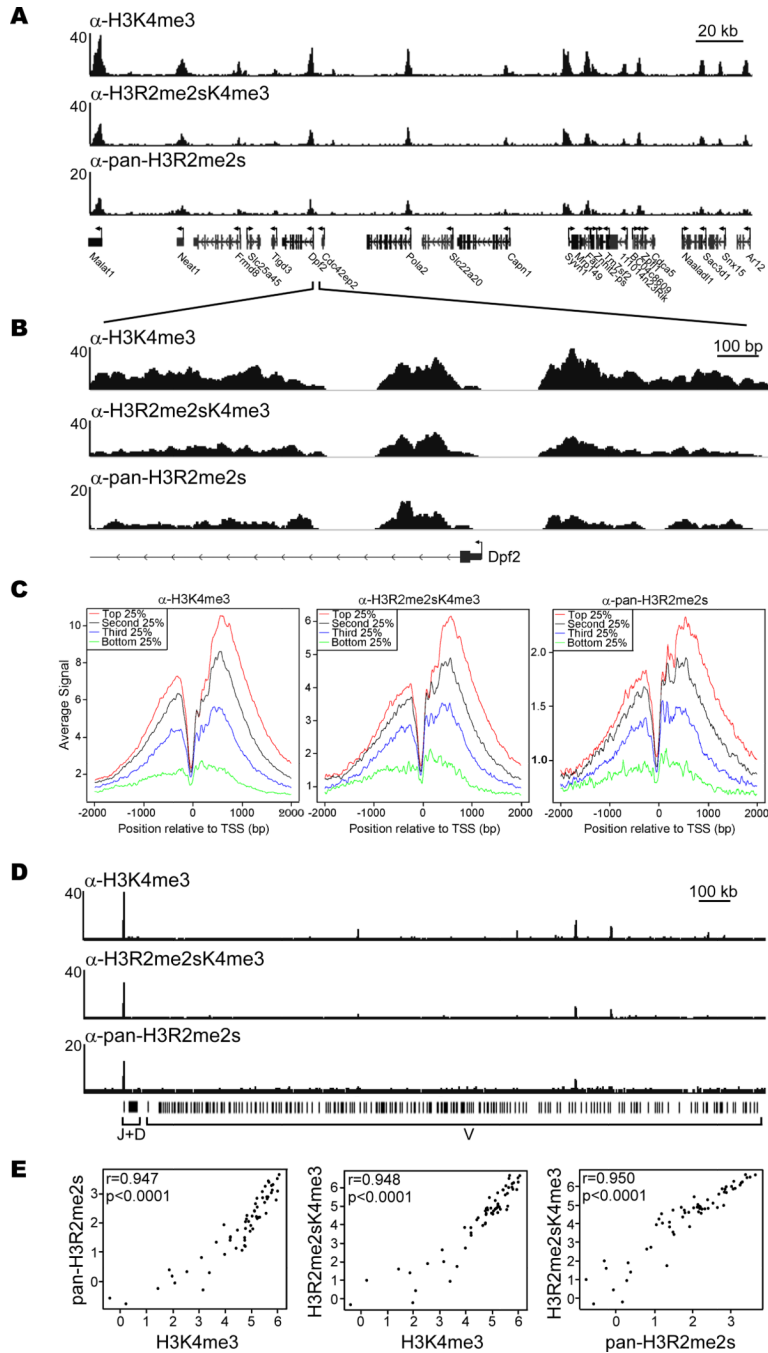


**Figure 2. H3R2me2s, H3R2me2sK4me3, and H3K4me3 are colocalized throughout the mouse genome**

(A) H3R2me2s is colocalized with H3K4me3 across a broad 350 kb region of murine chromosome 19. ChIP-seq analysis of H3K4me3 (top), H3R2me2sK4me3 (middle), and pan-H3R2me2s (bottom) enrichment in Rag2<sup>-/-</sup> Abelson-transformed pro-B cells. The transcription start sites, exons, introns, and relative orientations of the genes present in this 350 kb region are shown below the three panels.

(B) H3R2me2s is tightly colocalized with H3K4me3 near the transcriptional start site of Dpf2. A higher-resolution view of H3K4me3 (top), H3R2me2sK4me3 (middle), and pan-H3R2me2s (bottom) enrichment across a 1.75 kb region of murine chromosome 19. The

transcription start site (arrow), first exon (thick block), and part of the first intron (thin line) are shown below the three panels.

(C) H3R2me2s is present in two peaks flanking transcriptional start sites and is correlated with gene expression. The signal intensity of H3K4me3 (left), H3R2me2sK4me3 (middle), and H3R2me2s (right), averaged for all annotated murine genes, and plotted over a 4 kb window centered on the transcription start site. The genes are further stratified into four quartiles according to their expression levels in pro-B cells.

(D) H3R2me2s colocalizes with H3K4me3 at the murine IgH locus. H3K4me3 (top), H3R2me2sK4me3 (middle), and pan-H3R2me2s (bottom) enrichment across a 1.75 Mb region spanning the murine IgH locus. The relative positions of V, D, and J segments are indicated below the three panels.

(E) qPCR validation of the deep sequencing data. Chromatin from Rag2<sup>-/-</sup> Abelson-transformed pro-B cells was immunoprecipitated with the  $\alpha$ -H3K4me3,  $\alpha$ -H3R2me2sK4me3, or  $\alpha$ -pan-H3R2me2s antibodies. The enrichment of each modification relative to histone H3 was examined by qPCR using primers specific for 60 randomly selected promoters. The enrichment levels of H3R2me2s vs. H3K4me3 (left panel), H3R2me2sK4me3 vs. H3K4me3 (middle), and H3R2me2sK4me3 vs. H3R2me2s (right panel) were plotted for each of the 60 promoters. The Spearman's correlation coefficient and p-value for each combination are shown.

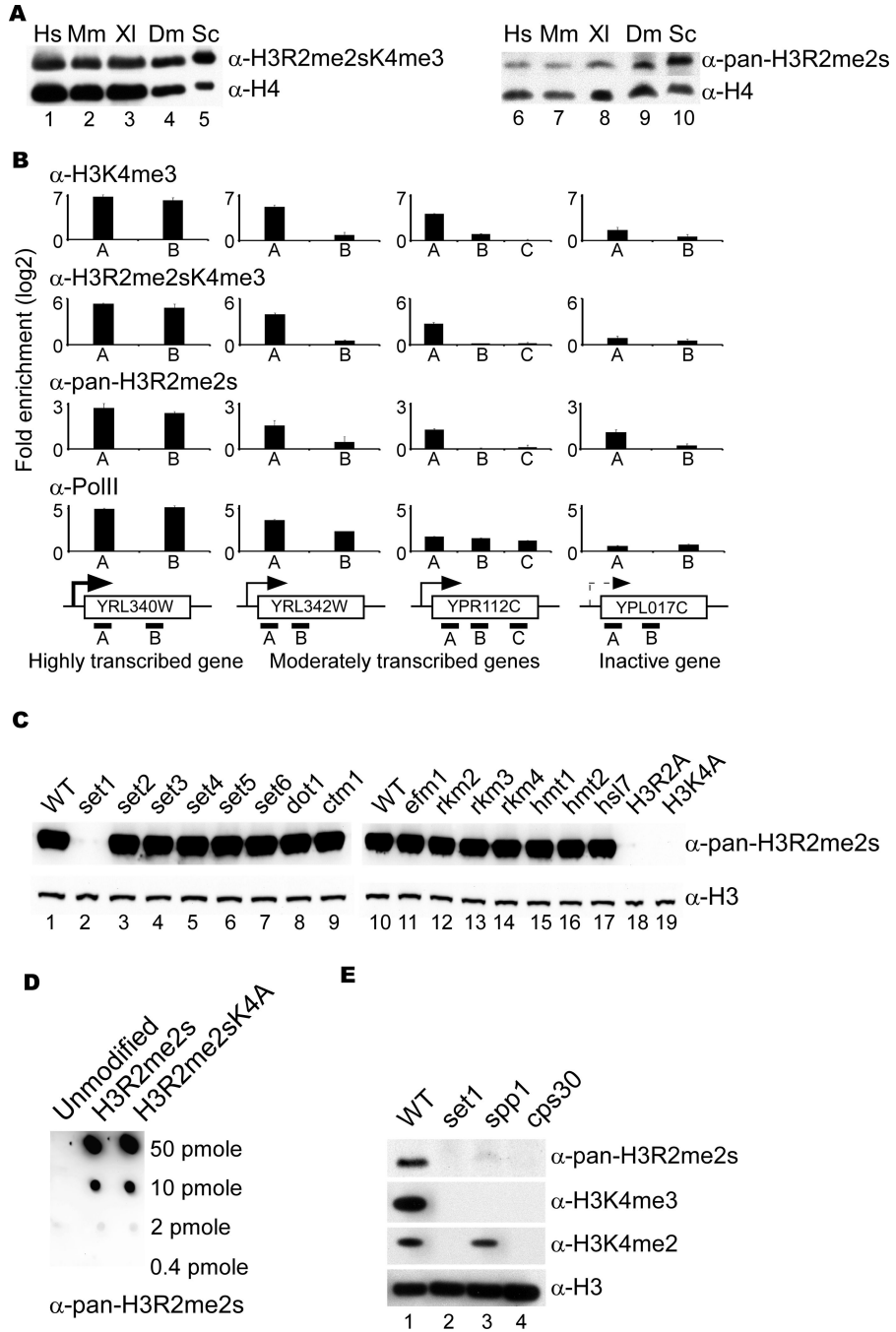


**Figure 3. H3R2me2s exists in *S. cerevisiae* and is intimately connected to H3K4me3**  
 (A) Evolutionary conservation of H3R2me2s and H3R2me2sK4me3. Nuclear extracts from human (Hs), mouse (Mm), frog (XI), fruit fly (Dm), and budding yeast (Sc) were subjected to Western blot analysis using the α-pan-H3R2me2s, α-H3R2me2sK4me3, and α-pan-Histone H4 antibodies.  
 (B) H3R2me2s, H3R2me2sK4me3, and H3K4me3 colocalize at representative yeast genes. *S. cerevisiae* chromatin was immunoprecipitated with the α-H3K4me3 (top panel), α-H3R2me2sK4me3 (second panel), α-pan-H3R2me2s (third panel), or α-Pol II antibodies. The enrichment of each modification relative to histone H3 was examined by qPCR using primers to a highly expressed gene, two moderately expressed genes, and a silent gene. The

schematic representations at the bottom of the graphs represent the genes that were analyzed and the locations of the qPCR primers within the genes. Results represent the mean  $\pm$  SD of three independent experiments.

(C) H3R2me2s is dependent upon Set1 and H3K4. Nuclear extract was prepared from wild type *S. cerevisiae* as well as several mutant strains, and subjected to Western blot analysis using the  $\alpha$ -pan-H3R2me2s  $\alpha$ -pan-H3 antibodies.

(D) The  $\alpha$ -pan-H3R2me2s antibody's recognition of symmetrically dimethylated H3R2 is unaffected by an H3K4A mutation. Indicated amounts of unmodified histone H3 (1–21), H3R2me2s, and H3R2me2sK4A peptides were spotted on PVDF membrane and probed with the  $\alpha$ -pan-H3R2me2s antibody.

(E) H3R2me2s is dependent upon Set1, Spp1, and Cps30. Nuclear extract from either wildtype, set1, spp1, or cps30 deletion mutant strains of *S. cerevisiae* were analyzed by Western blotting with the  $\alpha$ -pan-H3R2me2s,  $\alpha$ -H3K4me3,  $\alpha$ -H3K4me2, or  $\alpha$ -pan-H3 antibodies.